COMPUTER METHODS AND PROGRAMS IN BIOMEDICINE 137 (2016) 23–34

journal homepage: www.intl.elsevierhealth.com/journals/cmpb

A new approach to early diagnosis of congestive heart failure disease by using Hilbert–Huang transform

Gokhan Altan [a,*], Yakup Kutlu [b], Novruz Allahverdi [c]

[a] Mustafa Kemal University, Antakya, Turkey
[b] Iskenderun Technical University, İskenderun, Turkey
[c] KTO Karatay University, Konya, Turkey

ARTICLE INFO

Article history:
Received 16 September 2015
Received in revised form
3 August 2016
Accepted 1 September 2016

Keywords:
Congestive heart failure
Coronary artery disease
Hilbert–Huang transform
ECG
Multilayer perceptron
HRV

ABSTRACT

Congestive heart failure (CHF) is a degree of cardiac disease occurring as a result of the heart's inability to pump enough blood for the human body. In recent studies, coronary artery disease (CAD) is accepted as the most important cause of CHF. This study focuses on the diagnosis of both the CHF and the CAD. The Hilbert–Huang transform (HHT), which is effective on non-linear and non-stationary signals, is used to extract the features from R-R intervals obtained from the raw electrocardiogram data. The statistical features are extracted from instinct mode functions that are obtained applying the HHT to R-R intervals. Classification performance is examined with extracted statistical features using a multilayer perceptron neural network. The designed model classified the CHF, the CAD patients and a normal control group with rates of 97.83%, 93.79% and 100%, accuracy, specificity and sensitivity, respectively. Also, early diagnosis of the CHF was performed by interpretation of the CAD with a classification accuracy rate of 97.53%, specificity of 98.18% and sensitivity of 97.13%. As a result, a single system having the ability of both diagnosis and early diagnosis of CHF is performed by integrating the CAD diagnosis method to the CHF diagnosis method.

1. Introduction

An electrocardiogram (ECG) is a signal that records the electrical changes within the heart at regular intervals. Electrodes with different characteristics are used to obtain ECG signals (ECGs) from various parts of the body (arms, legs, chest, etc.). The horizontal plane of the ECG is time; the vertical plane is the amplitude of the electrical potential [1]. The ECG varies in frequency band from 0.5 Hz to 100 Hz and varies in amplitude value from 0 mV to 5 mV [2,3]. The ECG is used consistently for the monitoring and diagnosis of atrial and ventricular conduction disorders, rhythm disturbances and pericarditis, heart-related diseases and other systemic functions in the management of cardiac pacemakers [4]. The ECG has a very crucial role in monitoring and diagnosis of heart diseases. The ECG taken during the monitoring process is very important for the identification of abnormalities that may occur with complications. Therefore, the analysis, storage and transmission processes on the ECG in clinical applications have nowadays become intensively studied [5].

Electrical impulses occur as a result of polarization and depolarization. These impulses are presented as P, Q, R, S and T waves, as seen in Fig. 1 [6]. The sections between the waves are called segments; the distance between the waves is called an interval [1]. A P wave occurs as a result of the depolarization

* *Corresponding author.* Mustafa Kemal University, Antakya, Turkey. Fax: +90 (326) 613 56 13.
E-mail address: gokhan_altan@hotmail.com (G. Altan).

http://dx.doi.org/10.1016/j.cmpb.2016.09.003
0169-2607/

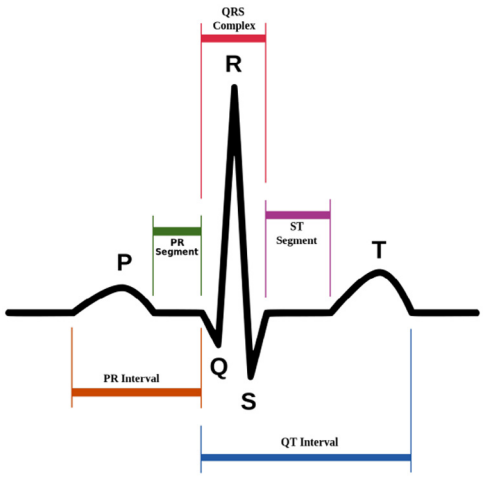

Fig. 1 – P, Q, R, S, and T waves on ECG.

of the atrium. The duration of the P wave is about 0.11 s and its amplitude varies from 0.18 mV to 0.22 mV in a normal derivation [7].

A QRS complex occurs as a result of the depolarization of the ventricle. The Q wave is the first negative wave and the R wave is the first positive one after the P wave. The S wave is the first negative wave after the R wave. The different QRS complex forms are seen in different derivations. The QRS complexes have significant meaningful differences even among normal subjects [8]. The QRS complex has the maximum amplitude in an ECG waveform. Duration of a QRS complex does not exceed 0.11 s and its amplitude is about 2–3 mV [7]. A T wave occurs as a result of the repolarization of the ventricles. The duration of the T wave may vary from 0.10 s to 0.25 s in a normal subject [8].

The studies in recent years have shown the significant relationship between autonomic nervous system (ANS) and cardiovascular cases. Heart rate variability (HRV) is a method for evaluating the ANS functionality of the sinus node level. The HRV is a measurement of the time-domain and the frequency-domain of beat-to-beat intervals. Beat-to-beat intervals are the length of time between two consecutive R waves. The time-domain methods usually use the avarage of normal-to-normal heartbeats. The frequency-domain methods are based on how the power of the ECG changes with a function of the frequency [9]. All the computable basic time-domain and the frequency-domain HRV measures were widely explained in the literature [9,10].

Congestive heart failure (CHF) is also known as heart failure. The CHF is a cardiac disease in which a heart does not have the ability to provide adequate metabolic cardiac output that a human organism needs. In the case of metabolic needs, the heart can increase the flow capacity by 200–600%. When the flow capacity of the heart is exceeded or increased, it cannot meet metabolic needs of subjects with CHF [11]. Doctors may recommend one or more of the following ways to diagnose the CHF: ECG, stress testing, echocardiography, B-type natriuretic peptide blood test, ejection fraction and cardiac catheterization.

Coronary artery disease (CAD) is a pathological condition where the diameter of the arteries decreases because of the cholesterol plaque on the heart wall. In this case, arteries cannot supply nutrients and oxygen to heart muscles [12]. He et al. [13] in the United States and Baldasseroni et al. [14] in Italy found that the CAD is the most risky factor for the CHF. This case has revealed the necessity for diagnosis of the CAD to early diagnosis of the risks for CHF. Doctors may recommend one or more the following ways to diagnose the CAD: ECG, stress testing, echocardiography, chest X-ray, blood tests (apolipoprotein A1, fibrinogen, urine albumin/creatinine ratio), coronary angiography and cardiac catheterization.

In literature, there are various methods to detect ECG disorders. Features were extracted by applying various methods to the ECG like diagnosing arrhythmia using morphological features of QRS complexes and R waves [15]. The features of these disorders were also extracted using wavelet transform [16,17]. Both wavelet transform and Fourier analysis were applied to ECG beats [18]. One method was used, morphological features of P, Q, R, S and T waveforms [19–21], whereas another worked on the phase space portraits of 3-lead ECG from subjects [22]. In addition, the template matching [23] and principal component analysis (PCA) methods [24,25] were used and both of them were applied to various signal processing problems. Many methods such as wavelet analysis, discrete Fourier transform, empirical mode decomposition (EMD), second order difference plot, wavelet packet decomposition are used to analyze nonlinear biomedical signals. One of the most well-known methods is the Hilbert–Huang transform (HHT) measurements. The HHT is a relatively new method used in biomedical data analysis. This transformation is applicable to non-linear and non-stationary signals. In recent studies, the HHT is applied to electroencephalography (EEG) signals to diagnose diabetes [26] and to predict epileptic seizure [27]. The HHT is also applied to audio signals for extracting features and filtering processes [28], the digital modulation classification for spectrum sensing [29], and to the ECG signals to diagnose atrial fibrillation [30] and the CHF [31]. In this study, HHT would be used to design an effective statistical feature extraction model using ECG to provide diagnosis and early diagnosis of the CHF. Thus, high-dimensional feature vectors that are formed in combination with instinct mode functions (IMFs) can be interpreted using the statistical analysis on the diagnosis and early diagnosis of the CHF.

The CHF and the CAD have been the subjects of some studies. A set of medical examinations and clinical tests are needed for the definitive diagnosis of the CHF. While some of the studies on CHF focused on determining the risk factor of death [32–34], some of them focused on the diagnosis of the CHF using the HRV measures [10,35,36]. The studies could separate CHF patients and normal subjects using the short-term HRV measures, wavelet entropy values, time domain measures and Poincaré plot measures [10], using the spectral analysis of HRV with autonomic changes model to diagnose risk of the CHF [32]; using features obtained applying wavelet transform and power spectral destiny (PSD) for R-R intervals [37]; using equal frequency in amplitude and equal width in time discretization [38]; using low and high frequency components, standard deviation (SD) of R-R intervals, daytime, nighttime and sub-maximal heart rate of HRV [34]; and using the features obtained applying linear discrimination analysis and the HRV measures [35]. Like the CHF, a set of medical examinations and clinical tests are needed for definitive diagnosis

of the CAD, too. They could separate the CAD patients and normal subjects using heart sounds [39]; the subjects' clinical data such as age, sex, heart rate, blood pressure [40]; Doppler ultrasound signals [41]; ventricle echocardiographic images [42]; and HRV measures [43–45].

As shown in the literature, HRV measures have usually been used on diagnostic studies of the CHF and a few of them have focused on raw ECG. As an alternative to studies in which HRV measures are used, this method provided greater sensitivity and higher accuracy performance with integration of diagnosis of the CHF and early diagnosis of the CHF by diagnosing the CAD in the same model using R-R intervals.

The aim of this study is to propose an alternative method to other studies that used various signal processing methods on the HRV measurements for the diagnosis and early diagnosis of the CHF. A noiseless 3 hour ECG form would be extracted to solve analysis problems in preprocessing. R-R intervals would be obtained from the extracted noiseless ECGs. The HHT would be applied to separated R-R intervals and IMFs would be extracted. The system would extract statistical features from the IMFs that are obtained applying the HHT to R-R intervals. Each instinct mode function (IMF) group obtained would be classified using multilayer perceptron neural network (MLPNN). The system would have a two stage classification model. In the first phase classification, it would separate the CHF and no-CHF subjects. In the second phase, it would diagnose the CAD and Normal subjects between no-CHF subjects. The classification performances of the diagnosis of the CHF, the CAD and the normal control group would be examined.

In the following sections, using the databases, the preprocessing of the ECG, the HHT method for feature extraction, the MLPNN classifier and derivation of classification performances were explained, and in the last section obtained results were discussed.

2. Materials and methods

ECG records were first taken in the structure of designing considered an early diagnosis system. We preferred moving the window analysis technique and segmented ECG data into 3 hour noiseless windows in the preprocessing because of noise and excessively long ECG records. R-R intervals of noiseless 3 hours in duration were used in the system. The IMFs were extracted applying the HHT and statistical features were calculated for the obtained IMFs in feature extraction. Statistical features were classified using an MLPNN. A detailed description of the system structure is presented in the following sections.

2.1. *Databases*

In literature, different databases including different diagnosis systems were used for the diagnosis of the CHF. The studies have generally focused on R-R intervals [10,35,36] while others have focused on [37] databases from the open source Physionet. Three different databases were used to diagnose CHF and CAD. These databases are the Normal Sinus Rhythm (NSR) Database, the CHF Database and the Long-Term ST Database.

The first database group [46] includes the NSR database and the CHF database and used to diagnose the CHF. It includes 54 long-term ECGs of subjects that included 30 men, aged 28.5 to 76, and 24 women, aged 58 to 73 in the NSR. It also included 29 long-term ECGs of subjects aged 34 to 79 and included 8 men and 2 women and 21 individuals of unknown gender all with CHF. The individual recordings of databases are about 24 hours in duration. The ECGs were digitized at 128 samples per second.

The second database group includes the Long-Term ST Database [47]. The Long-Term ST database contains 86 long-term ECGs from 80 subjects, chosen to exhibit a variety of events of ST segment changes. There are 26 CAD subjects labeled as undiagnosed and 60 CAD subjects labeled as diagnosed in this database. The individual recordings of the Long-Term ST database are between 21 and 24 hours in duration, and contain two or three lead-ECGs.

Lead I-ECG type is selected in this study. Characteristics of Lead I are the same in both first group and second group databases. Each ECG has been digitized at 250 samples per second.

2.2. *Preprocessing*

In each group of databases, the sampling rates are the same. But when the diagnoses of the CHF and the CAD are integrated into one system, an analysis problem occurs because of the large number of samples. Therefore, we would like to call attention to the fact that all data records are obtained from the Physionet databases used as R-R intervals. As we mentioned in the introduction, an ECG has 6 waves. The dominant peaks on an ECG are R-waves. Sometimes, other waves may not be recorded because of physical and recording conditions. Due to this characteristic of R waves, it is easy to be detected on an ECG. In addition, an ECG has a signal characteristic that can be easily affected. But R-R intervals are less affected by noise in an ECG signal. R-R intervals assess an estimate of cardiac output. These characteristic features of R-R intervals are the reason for extracting R-R intervals instead of using the raw ECG in this study.

The information in a biomedical signal is unevenly distributed. Dispersion of signals can be expressed as bandwidth correlating with detected wave forms [48]. Therefore, the non-uniform R-R intervals that are obtained from the ECG allow decreasing sample size by eliminating the less important signal parts while the characteristic features remain well represented. So, we extracted R-R intervals that have a 128 Hz sampling rate using PhysioToolkit software [46] from the three databases. The PhysioToolkit software has an ability to detect P, Q, R, S, T waves and QRS complexes, and to extract R-R intervals from the raw ECG and can convert them to MATLAB files.

Analysis problems occurred because signals were too long during the transformation processes. There was much noise. The noise in an ECG may be correlated with the physical activity, recording conditions or heart rate symptoms. These conditions occur as a result of the long length of the R-R interval time. R-R intervals vary in length from about 0.7 to 0.9 seconds. We coded a class which controls if the R-R interval segment has a time that is longer than 0.9 second and shorter than 0.7 second. If the case is true, the code restarts to select a noiseless segment until a 3 hour R-R interval is extracted. Therefore, 3 hour noiseless ECGs were extracted from the raw

ECGs. R-R intervals were obtained from the selected 3 hour noiseless ECGs. The IMFs were extracted by applying the EMD to each extracted noiseless R-R intervals. Hilbert transform (HT) was applied continuously to each IMF and the Hilbert spectral analysis (HSA) is plotted from the signals which were obtained with the same number of the IMFs.

2.3. *Hilbert–Huang transform*

The HHT is one of the effective ECG analysis techniques which include both the EMD and the HT. The HHT is an adaptive analysis method on both the ECG and R-R intervals which are non-stationary and non-linear signals. The mathematical algorithm of the method could not be defined clearly due to the flexibility of the stoppage criterion [27]. The HHT consists of a two-step analysis. The first step is the EMD. The EMD extracts IMFs which are frequency-modulated signals about processes. The instantaneous frequency and amplitude values in the time-frequency domain are extracted from each obtained IMF by applying the HT. The HHT provides more distinctive, clear and precise results than any other method for non-linear and non-stationary signals [49]. Considering all these characteristics, our work focuses on the HHT analysis on non-uniformly sampled R-R intervals.

2.3.1. *Empirical mode decomposition*

The EMD is a flexible analysis method that is used for non-linear and non-stationary processes. The most important characteristic that separates this algorithm from the other transformations is the ability of producing oscillations apart from the signal by assuming a random signal which consists of its own self oscillation mode at different frequencies. Each oscillation is symmetrical relative to the local mean of the local extreme. Each oscillation is indicated by an IMF that is an amplitude/frequency modulated signal. All IMFs from a signal form a complete and nearly orthogonal basis for the original signal. IMF is selected to provide the following two basic conditions [29,49]: (1) in the whole dataset, the number of extrema and the number of zero-crossings must be either equal or differ at most by one, and (2) at any t time at signal, the mean value of the envelope defined by the local maximum and the envelope defined by the local minimum must be equal.

Due to the success of the EMD on non-linear and non-stationary signals, the boundary problem and mode mixing problem are the basic defects on finite time series. The maximum and minimum envelopes with cubic spline function are distorted badly because of divergence on both the end point of the signal and inside signal. Various methods were proposed to solve the defect and the boundary problem, such as neural network model [50], autoregressive models [51] and local self-similarity functions [52]. In this study, an efficient similarity model is utilized to obtain spline interpolation and it is described in detail in [52].

Specified conditions are that extract IMFs are used to prevent the negative frequency formation and to keep instantaneous frequency of the narrow band signal on the band while calculating the instantaneous frequency with the HT. The mean value of the envelope defined using the local maximum values and the envelope defined using the local minimum values are used to calculate the local mean. The local maximum, local minimum and local mean are shown in Fig. 2. A new form of the signal is obtained by subtracting the calculated local mean from the original signal. This new form of the signal is controlled if it satisfies the basic conditions of the IMF. If it does not satisfy the conditions, the local mean value is recalculated by using the local maximum and local minimum values of the new form of the signal. This procedure is repeated until a new form of the signal satisfies the conditions obtained by the IMF. When The IMF is extracted, the residual signal is extracted by the IMF from the original signal and the same IMF extraction processes are continually repeated for the residual signal until obtaining a monotonic function for the whole signal [53]. The EMD has a detailed formula calculation in literature [27,29,49].

$$X(t) = \sum_{j=1}^{n} c_j + r_n \tag{1}$$

It is not possible to extract new IMF from the residual signal when it has only one local extreme or obtains only one monotonic function for the whole signal. In this case, the EMD process ends. In Equation (1) c represents the number of extracted IMFs, r_n represents the residual signal and n represents the repetition number of the algorithm steps [27]:

Straightforward implementation of sifting process produces mode mixing problems due to the IMF restitution. Different IMFs may be extracted for same signal in the EMD process because of the intermittency signals with high frequecy, signal loss, and noises. The unfixed feature extraction stages results with big problems for classification stages of the pattern

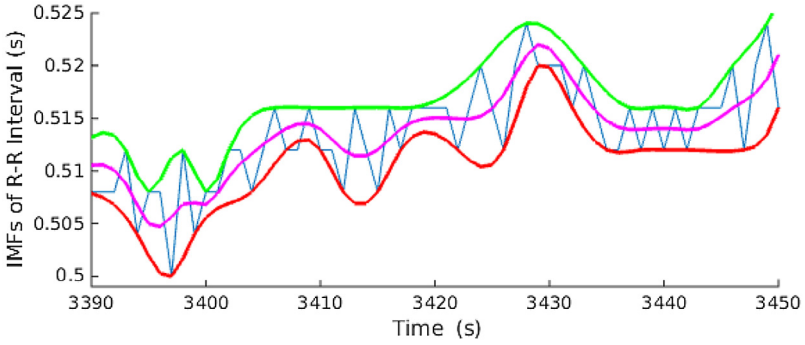

Fig. 2 – A randomly selected part of the EMD process on the IMFs of R-R intervals from a random CHF patient.

recognition algorithms. When we tested some of the random R-R interval time series with the traditional EMD algorithm, we did not meet any mode mixing problem, even so we utilized the Ensemble EMD model to avoid the possible noises that would produce mode-mixing problem. The Ensemble EMD is the mean of the corresponding IMFs that are obtained with traditional EMD by adding white noise series cancel each other signal at each stage of adaptively and locally decomposition. A unique residue signal is calculated for decomposing each mode. Adding white noise series procedure continues until the IMF approximates to the required IMF [54].

2.3.2. *Hilbert transform*

The most important and initial feature of non-linear signals is inherent wave frequency modulation that shows the instantaneous frequency value in one cycle. Instantaneous frequency values give the signal characteristics in the most comprehensible way. The HT is a process for computing the instantaneous frequency characteristics of the signal [27,49]. The complex conjugation of a real-valued $x(t)$ function that is applied to the HT equals the $y(t)$ function.

$$y(t) = H[x(t)] = \int_{-\infty}^{\infty} \frac{x(\tau)}{t-\tau} d\tau \tag{2}$$

The analytical $x(t)$ function can be written by using the HT as follows:

$$z(t) = x(t) + jy(t) = a(t)e^{j\theta(t)} \tag{3}$$

The instantaneous amplitude and phase functions of expressed formula above are as follows:

$$a(t) = \sqrt{x^2(t) + y^2(t)} \tag{4}$$

$$\theta(t) = arctan\left(\frac{y(t)}{x(t)}\right) \tag{5}$$

The instantaneous frequency information can be obtained from the functions above:

$$\omega(t) = \frac{d\theta(t)}{dt} \tag{6}$$

$$f(t) = \frac{1}{2\pi}\frac{d\theta(t)}{dt} \tag{7}$$

The analytical expression of $x(t)$ can be obtained by applying the HT to each IMF that is extracted after applying the EMD to the $x(t)$ signal. The instantaneous frequency and amplitude values of each IMF can be calculated with the help of Equations (4)–(7):

$$x(t) = \mathbb{R}\left\{\sum_{i=1}^{n} a_i(t)e^{j\omega_i(t)dt}\right\} \tag{8}$$

Equation (8) indicates that each IMF is the amplitude or frequency modulated signal. The EMD performs an exceedingly good parsing process by analyzing the signal in various amplitude and frequency scales for non-stationary signals [27]. The amplitude of the frequency-time distribution (ω) is called the HSA. The marginal spectrum can be calculated by using the HSA [27,49].

$$h(\omega) = \int_0^t H(\omega, t)dt \tag{9}$$

3. Classifier and performance evaluation

The MLPNN is a learning model that calculates the output value(s) using input values, conventional neuron weights or randomly taken weights. The most important phase of the learning model is called training. The training phase is carried out to obtain the output weights, calculated input values and available neuron weights equal to zero. But this case cannot always be performed. The main aim in the MLPNN is obtaining the minimum error between the actual output value(s) and calculated output value(s). The neuron weights are adapted using learning rate and learning algorithms during the training phase. Some of the advantages of the MLPNN include the ability of using the results in a condition known to decide about unknown situations and the high degree of efficiency and reliability that determines the validity of the systems [55].

$$x_o = \varphi\left(\sum_k (x_k w_{ko})\right) \tag{10}$$

In Equation (10) where $\varphi()$ is activation function, x_k, the value of k number node and w_{ko} is the weight of connection between the k number node and y output.

The MLPNN has the most widely used network architecture in pattern classifications. The MLPNN has an input layer, hidden layer(s) and an output layer (Fig. 3). Each layer may have various numbers of neurons depending on the complexity of the problem. Every neuron has been weighted to the average of the inputs through the activation function. The most commonly used activation function in the MLPNN is sigmoid [56].

Some of the statistical computations had to be used in validation of medical diagnosis systems [30,55]. Accuracy (ACC), Specificity (SPE) and Sensitivity (SEN) are used to evaluate performance of the designed system.

$$SEN = \frac{TP}{TP + FN} \tag{11}$$

$$SPE = \frac{TN}{TN + FP} \tag{12}$$

$$All\ ACC = \frac{\sum_{i=1}^{N} TP_i}{All\ beats} \tag{13}$$

In the Equations (11)–(13), TP (True Positives) is the number of signals with the required correct specifications; TN (True Negatives) is the number of other signals correctly classified; FP (False Positives) is the number of signals with the required specifications incorrectly classified; and FN (False Negatives) is the number of other signals incorrectly classified by the designed integrated system.

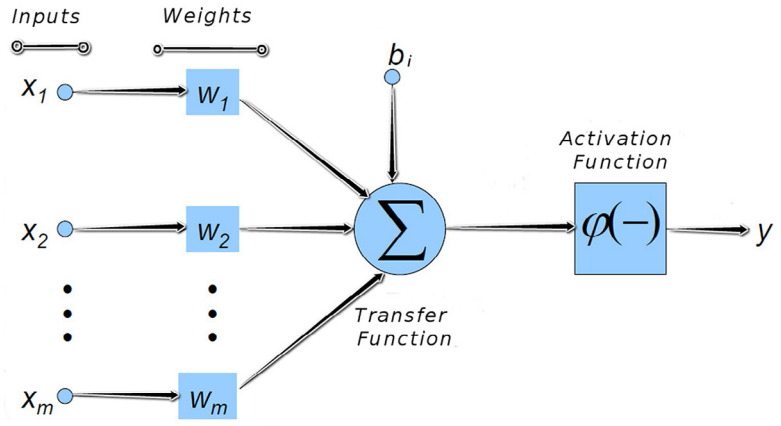

Fig. 3 – Structure of the artificial neural network.

4. Experimental results

The various signals (ECG, EEG, etc.) of diseases are analyzed with digital signal processing methods in medical diagnosis systems. In the literature, the raw ECG and the HRV measures have been the primarily used signals in the diagnosis of heart diseases. In this study, R-R intervals are used to make the diagnosis of the CHF and early diagnosis of the CHF by the diagnosis of the CAD or a normal group (Fig. 4).

When the ECG signals in three databases are analyzed, it is seen that the ECG signals are noisy and too long for analysis. The noisy parts of signals distort some features of the patient's disease. Long-time (24 hours) R-R intervals might not be necessary to analyze conditions on an ECG, as the analysis of the short-time HRV might be sufficient and more effective. The length of the selection of the short segments from the original R-R intervals is a situation that should be tested with various lengths. When we tested with 24 hour long-time HRV, it caused analysis problems like long time or endless calculations. According to the recommendations in the literature for the short-term HRV [9], a 5 min short-time HRV is commonly used. In our experiments, when the HHT with the addition of white noise in each ensemble member has an SD of 0.1 in the EMD was applied to 5 min R-R intervals, IMFs ranging at least 7 and 8 were obtained. Statistical features have a low performance (seen in Table 1) for this diagnosis system. IMFs ranging at least 10 and 13 obtained from 3 hour R-R intervals in duration are seen in Table 2. The higher classification performances were achieved using 3 hour R-R intervals. In light of this situation, meaningful parts were lost for diagnosing CHF when R-R interval was segmented into such short forms.

Table 1 – Accuracy, sensitivity and specificity achievements of diagnosis of CHF with 5 min R-R intervals.

	IMF1	IMF2	IMF3	IMF4	IMF5	IMF6	IMF7	$r(x)$
SEN	56.67	45.56	42.96	33.70	34.44	67.78	25.19	40.00
SPE	66.21	55.17	68.97	65.52	84.83	46.21	38.62	54.48
ACC	60.00	48.92	52.05	44.82	52.05	60.24	29.88	45.06

This study reached better performances in both the diagnosis of the CAD and the CHF by using 3 hour length R-R intervals. Therefore, we discussed separating noiseless 3 hour ECG forms to solve analysis problems in the preprocessing. R-R intervals were obtained from 3 hour noiseless ECGs on all three databases. The EMD is an analysis method that takes the whole signal as an input to indicate the IMFs. So, a sample size of

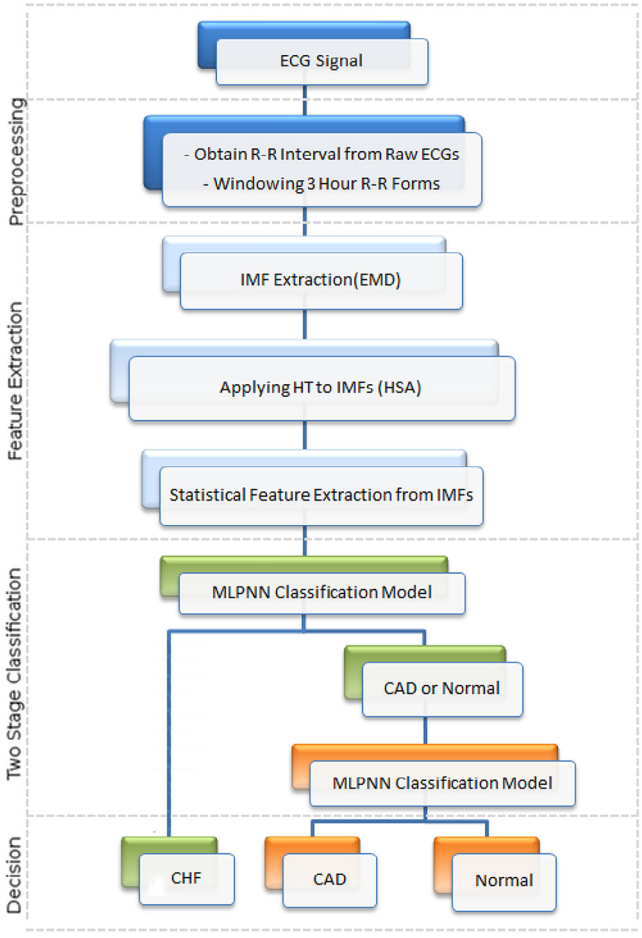

Fig. 4 – Structure of proposed diagnosis system.

Table 2 – Accuracy, sensitivity and specificity achievements of diagnosis of CHF with 3 hours R-R intervals.

	IMF1	IMF2	IMF3	IMF4	IMF5	IMF6	IMF7	IMF8	IMF9	IMF10	$r(x)$
Sensitivity	74.07	79.26	100.00	97.41	92.22	84.07	85.71	85.56	72.59	78.89	84.98
Specificity	62.07	80.00	93.79	90.34	81.38	71.03	77.77	75.17	67.59	66.21	76.54
Accuracy	69.88	79.52	97.83	94.94	88.43	79.52	82.63	81.93	70.84	74.46	82.00

the processing window in the EMD with 10 800 of datapoints for 3 hour length R-R intervals is utilized in analysis process. The EMD was applied to separate R-R intervals and the IMFs were extracted. R-R intervals obtained from the NSR and R-R intervals obtained from the CHF subjects and some of the obtained distributions of the IMFs extracted by applying the HHT are shown in Fig. 5.

Various numbers of IMFs ranging from at least 10 and at most 14 were extracted for each R-R interval for 169 subjects from three databases. Various numbers of IMFs may cause analysis problems in the designed system when IMFs were grouped according to the number. So, analysis of the IMF groups is impossible, because of various numbers of the IMFs. We need the same size of features set for proper classification. We cannot ignore the last few IMFs (numbered 11–14) because they may have a significance in the diagnosis of the CHF. Therefore, we extracted the first 10 numbers of IMFs and we summed up the remaining IMFs from IMF 11 to the last as $r(x)$.

$$X(t) = \sum_{j=1}^{10} c_j + r(x) \tag{14}$$

$$r(x) = \sum_{j=11}^{end} c_j + r_n \tag{15}$$

The HSA was used for examining each IMF's instantaneous frequency as functions of time by applying the HT. The HT allows deriving the analytic representation of a signal and includes the phase information that depends on the phase information about signals. As a result of the HSA, the frequency-time distribution of signal amplitude which permits the identification of localized features is obtained (seen in Fig. 6).

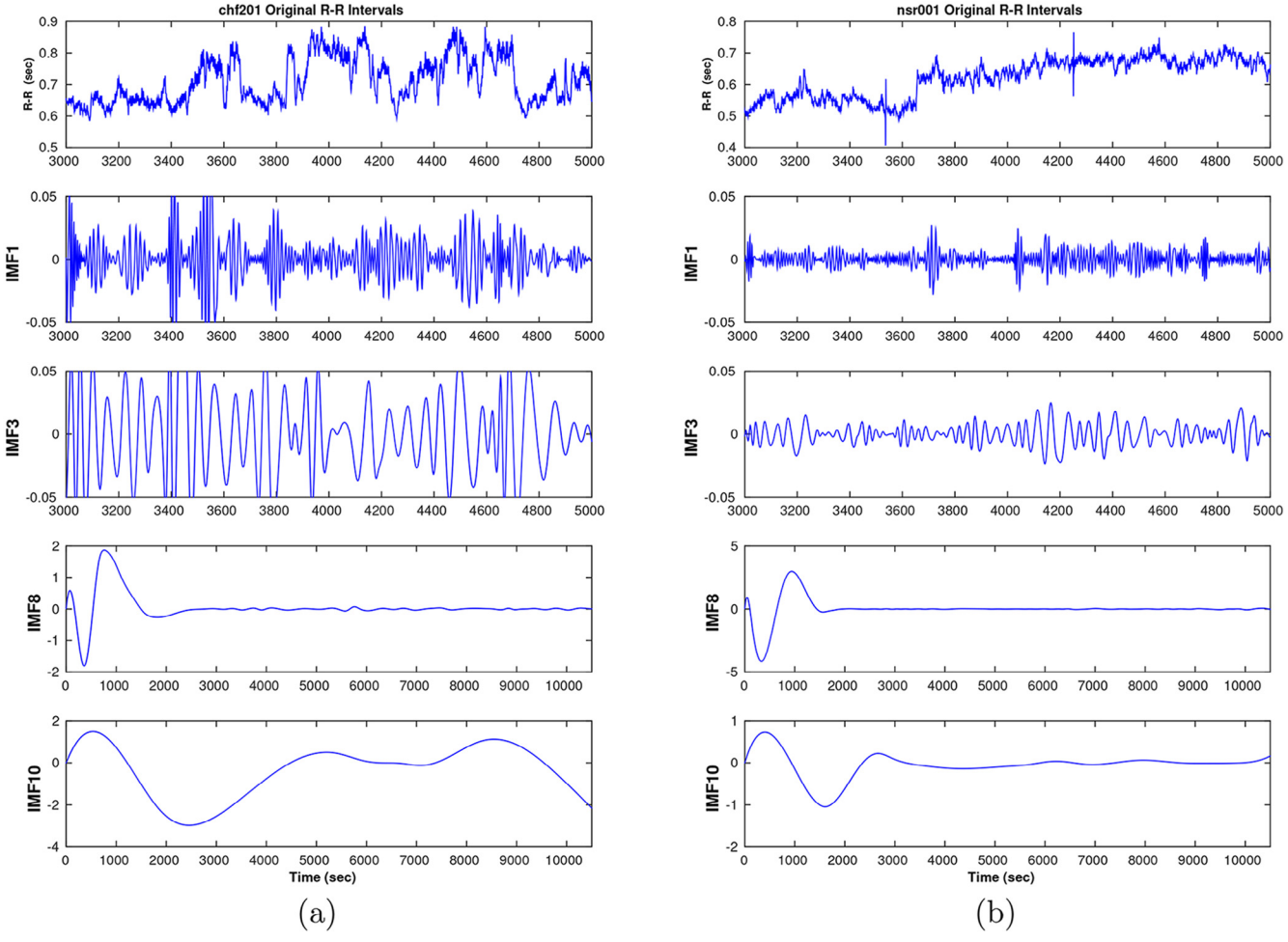

Fig. 5 – Randomly selected R-R intervals and samples of IMFs distribution: (a) R-R intervals obtained from subject with the CHF and some of IMFs, (b) R-R intervals obtained from the NSR subject and some IMFs.

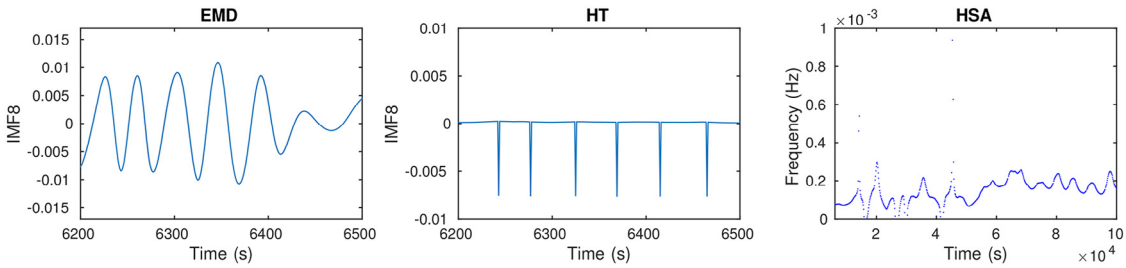

Fig. 6 – Obtaining frequency-time distribution from IMF 8, the EMD (random segment of IMF8), the HT (random segment of applying the HT to IMF8), the HSA of IMF8.

Applying the HT, statistical features were extracted from each IMF and a dataset was created by combining the statistical features of each IMF signal. Nine statistical features, minimum (Min), maximum (Max), skewness (Skw), median, mean, SD, avarage correlation (Corr), mode and energy of IMFs, were calculated. The statistical features are calculated with the default parameter values using Matlab 2014b. The Pearson method is the default type for linear correlation. We correlated each signal with all other signals in same class and utilized average of the correlation values as the feature. As seen in Tables 3 and 4, correlation is the highest responsible feature; mod is the lowest responsible feature for reducing HRV in both the CHF and the CAD patients.

The MLPNN classifier was trained using the back-propagation algorithm. The model has one input layer with 9 statistical inputs, 2 hidden layers and uses the sigmoid activation function. The first hidden layer has 6 neurons and the second hidden layer has 2 neurons. Each neuron has an associated connection with neurons on adjacent layers. We preferred the hyperbolic tangent sigmoid function due to its effectiveness and ease in calculating the derivation of updating input weights during diagnosis of the CHF. We preferred the back propagation network due to its advantages of intuitive approaches, providing evolutionary optimization by both forward and backward pass transfers on learning algorithms.

This system was tested using 5-fold cross validation. In this method, a whole dataset is randomly divided into 5 parts. It has been noted that each randomly divided part has an equal number of uniform distributions on subjects. In every classification, one of these parts was selected as test data and the other four parts were combined as a set of training data for the MLPNN system and the performance achievements of the system were investigated. SEN, ACC and SPE parameters are the test characteristics that are the basis of independent testing and diagnosis of diseases in a general population in medical diagnostic systems [26,55]. These test characteristics were calculated for 5 times for each part of the dataset and mean values were calculated for the results. Thus, we provided the use of all obtained statistical features as test sets except the sets used for training. Results were tested on all situations of system [57]. High accuracy performance was achieved using extracted statistical features of the MLPNN classified model. Besides the high accuracy performance, sensitivity and specificity calculations that determine the overall success and reliability of system were achieved, too.

We used a two-stage classification. Both two stages have the same neural model. In the first stage classification, the system separates subjects as CHF and no-CHF (the CAD + Normal). In the second stage classification, subjects were classified as CAD and Normal. The MLPNN used in the system has 9 inputs. Nine statistical features for each IMF were given as inputs to the model. The system has one output that is triggered by the sigmoid function.

The dispersion of performance evaluation values was obtained by using the CHF Database and the NSR Database as seen in Fig. 7. There were several achievements using this system; CHF patients were separated from no-CHF subjects with a classification accuracy rate of 97.83%, a specificity of 93.79% and a sensitivity of 100% using statistical features from IMF 3 extracted applying HHT to R-R intervals. Corr is highly responsible for reduced R-R intervals in the diagnosis of the CHF as seen in Table 5.

The dispersion of performance evaluation values that were obtained by using the Long-Term ST database is seen in Fig. 8.

Table 3 – Performance of each statistical features for reduced R-R intervals in CHF patients.

	Corr	Energy	SD	Max	Min	Skw	Mean	Median	Mode	All
SEN	93.71	89.63	88.51	86.29	80.37	60.37	40.01	34.07	24.81	100.00
SPE	66.21	67.58	57.24	55.86	46.89	51.03	60.02	49.65	42.06	93.79
ACC	84.09	81.92	77.59	75.66	68.67	57.10	46.98	39.51	30.84	97.53

Table 4 – Performance of each statistical features for reduced R-R intervals in CAD patients.

	Corr	Energy	SD	Min	Max	Skw	Mean	Median	Mode	All
SEN	90.01	80.00	75.19	67.78	62.96	48.15	35.56	22.96	18.89	97.13
SPE	84.83	93.10	75.17	66.21	56.55	61.38	53.79	57.93	48.97	98.83
ACC	88.19	84.58	75.18	67.23	60.72	52.77	41.93	35.18	29.40	97.53

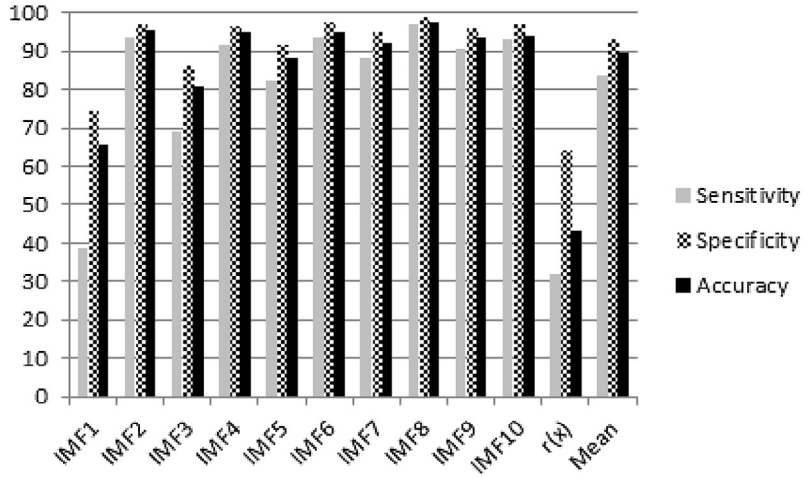

Fig. 7 – Performance graph of the CHF diagnostic.

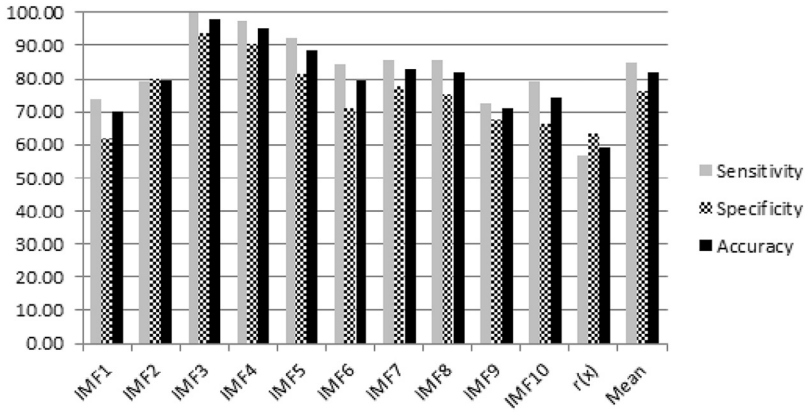

Fig. 8 – Performance graph of CAD diagnostic.

There were several achievements; CAD patients were separated from other subjects with a classification accuracy rate of 97.53%, a specificity of 98.83% and a sensitivity of 97.13% using statistical features from IMF 8 extracted by applying the HHT to R-R intervals. Corr is a highly responsible feature for reduced R-R intervals in diagnosis of the CAD as seen in Table 6.

Considering all the results, the HHT can perform the separation process for medical diagnosis systems by providing analysis of non-stationary and non-linear R-R intervals in various amplitude and frequency scales. Neural network classification using statistical features extracted from the new noiseless R-R signals has reached a high success rate of accuracy and sensitivity. This study shows that extracted features using the HHT can be used as an alternative method to long-time and short-time HRV measurements [10,35,36,43–45], Poincaré plot measurements [10,44], wavelet coefficients and wavelet entropy features [10,45].

Table 5 – Accuracy, sensitivity, specificity achievements for reduced R-R intervals in CHF patients.

	Corr	Energy	SD	Median	Max	Skw	Mean	Min	Mode	All
SEN	93.71	89.63	88.51	86.29	80.37	60.37	40.01	34.07	24.81	100
SPE	66.21	67.58	57.24	55.86	46.89	51.03	60.02	49.65	42.06	93.79
ACC	84.09	81.92	77.59	75.66	68.67	57.10	46.98	39.51	30.84	97.53

Table 6 – Accuracy, sensitivity, specificity achievements for reduced R-R intervals in CAD patients.

	Corr	SD	Energy	Median	Skw	Mean	Min	Max	Mode	All
SEN	90.01	80.00	75.19	67.78	62.96	48.15	35.56	22.96	18.89	97.13
SPE	84.83	93.10	75.17	66.21	56.55	61.38	53.79	57.93	48.97	98.83
ACC	88.19	84.58	75.18	67.23	60.72	52.77	41.93	35.18	29.40	97.53

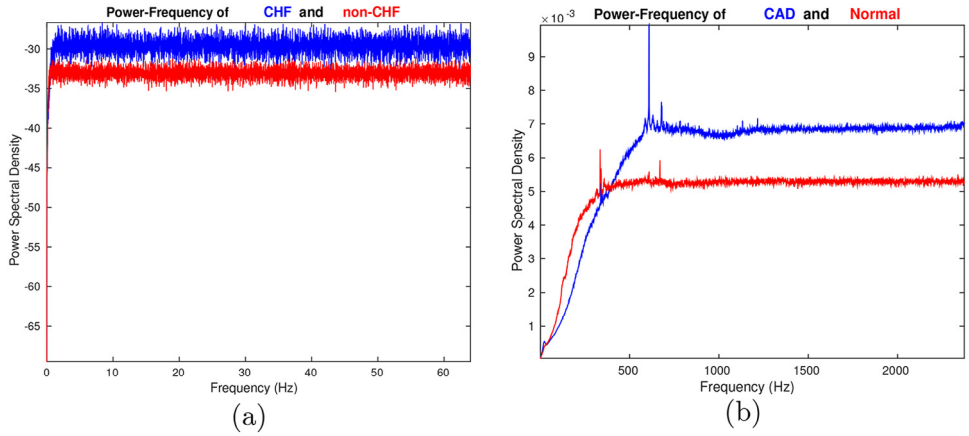

Fig. 9 – Frequency-power spectrum density plots (a) corresponding to 8th IMFs for CHF patients, (b) corresponding to 3rd IMFs for CAD patients.

In this study, we calculated the average PSD of the CHF, no-CHF, the CAD and Normal patients. It is clear that the frequency-PSD corresponds to the 3rd and 8th IMFs for the CHF (Fig. 9a), and the max, min, SD and the power-frequency features for the CAD diagnosis (Fig. 9b) are on different spectrums.

A comparison of the CHF diagnosis studies in the literature is seen in Table 7. Extracted features, accuracy, specificity and sensitivity performance measurements are given. All studies used the same subject numbers and same databases.

A comparison of the CAD diagnosis studies in the literature is shown in Table 8. Extracted features using these databases and the values of Accuracy, Specificity, Sensitivity performance measurements are also given. Because of the different databases, the number of subjects is given in Table 8.

When IMF groups, extracted by applying the HHT to R-R intervals, were used in designing the MLPNN, the performance achievements reached an accuracy rate of 97.83%, a specificity rate of 93.79% and a sensitivity rate of 100% using IMF 3 in the diagnosis of the CHF. For non-subject with a diagnosis of CHF and diagnosis of CAD, the most important risk factor for the CHF is the diagnosis of CAD. So the early diagnosis of CAD was achieved with an accuracy rate of 97.53%, a specificity rate of 98.83% and a sensitivity rate of 97.13% using IMF 8. Thus, in addition to diagnosing the CHF, the early diagnosis of CHF by the diagnosis of CAD is provided for other risk group subjects.

The CHF is one of the leading causes of death and cardiac dysfunction, and strongly related with the CAD. It is important to improve the CHF diagnosis systems to prevent mortality and morbidity rates and have greater and healthy lifetime benefits. The narrowing of the coronary artery limits the blood supply in the CAD and this condition usually results to CHF in the future [58]. It is a good way to diagnose the CAD as early diagnosis of the CHF, in order to delay the diagnosis of the CAD. The proposed method suggests high performances for both diagnosis of the CHF and the early diagnosis of the CHF by detecting the CAD.

5. Conclusion

We used three databases that have a wide use in the literature. New noiseless short-time ECG waveforms were obtained from the databases and R-R intervals were extracted. The proposed system was used for the diagnosis and early diagnosis

Table 7 – Comparison of the CHF classification performance with related studies.

Authors	ACC	SPE	SEN	Database	Features
Isler and Kuntalp [10]	96.39	94.74	100	CHF-R-R, NSR-R-R	HRV measures, Poincaré measures, wavelet entropy
Asyali [35]	93.24	98.08	81.82	CHF-R-R, NSR-R-R	Long-term HRV measures
Pecchia et al. [36]	96.40	100	89.70	CHF-R-R, NSR-R-R	Short-term HRV measures
This study	97.83	93.79	100	CHF-R-R, NSR-R-R	Statistical features of obtained IMFs after HHT

Table 8 – Comparison of CAD classification performance in literatures.

Authors	ACC	SPE	SEN	Subjects	Features
Lee et al. [43]	85–90	-	-	61/82 (Normal/CAD)	HRV measures, Arterial wall thickness
Kim et al. [44]	75.00	81.80	72.50	20/64 (Normal/CAD)	Frequency-domain measures of HRV, Poincare measures
Giri et al. [45]	96.80	93.70	100	10/15 (Normal/CAD)	HRV measures, Wavelet coefficients
This study	97.53	98.83	97.13	25/61 (Normal/CAD)	Statistical Features obtained from IMFs

of CHF. So, the integrated system with the diagnosis of CHF and CAD used for early diagnosis of CHF was designed. In this integrated system, the MLPNN was used for classifying the statistical features of IMF groups extracted applying the HHT. Accuracy, specificity and sensitivity achievements were used to evaluate system performance.

Fig. 7 and Fig. 8 depicted an accuracy rate of 97.83%, a specificity rate of 93.79% and a sensitivity rate of 100% achieved in the diagnosis of CHF, and an accuracy rate of 97.53%, a specificity rate of 98.83% and a sensitivity rate of 97.13% achieved in the diagnosis of CAD. Therefore, in the early diagnosis of CHF, statistical features of IMFs were extracted applying the HHT to R-R intervals.

As it is seen in Table 7 and Table 8, the diagnosis of CHF is achieved with a higher accuracy rate and sensitivity rate than related works on the same databases. It is hard to compare the diagnosis accuracy of this study with others because of the different numbers of subjects and different databases. Nevertheless, the most important feature that makes this study superior to others is the diagnosis of CAD, as the early diagnosis of CHF having high rates of accuracy and sensitivity. This work provides the integration of two diagnostic systems into a single system. The analysis time of the diagnosis of both disabilities varies between 2s and 6s. This characteristic of the processing and decision time makes the proposed HHT-based analysis method a real-time applicable method in early the diagnosis of the CHF and diagnosis of the CHF. In future works, a real-time model would be performed for early diagnosis of CHF and the genetic search feature selection algorithms will be used to enhance, the classification accuracy rate and leave one out cross validation algorithm will be used to design a patient-independent system.

Common signal processing methods have an approval overview of the temporal and frequency precision of the linear and stationary signals; the HHT has the ability to extract the characteristic information that indicates the different frequency and the energy bands of stiffness in the processing of non-linear and non-stationary signals. R-R interval time series are the non-linear and non-stationary signals which are less affected type of the ECG by noise and frequently used in cardiac diseases such as CHF and CAD [10,32]. The most remarkable advantages of the HHT are providing the frequency value as a function of the time with an adaptive way and estimating both the subtle changes and relative suppressions of power at a specific frequency from the instantaneous frequency of the R-R intervals time series of time-varying. Extracted IMFs from the R-R intervals time series are employed the base of the instantaneous frequency and instantaneous bandwidth of the components by the HT. The proposed method proved to be an efficient way to diagnose CHF and the early diagnosis of CHF by detecting CAD using the HHT-based statistical features from short-term R-R intervals time series.

Acknowledgments

We would like to thank the anonymous reviewers for their patience and extremely cautious proofreading of this paper.

REFERENCES

[1] M. Gabriel Khan, Rapid ECG Interpretation (Contemporary Cardiology), third ed., Humana Press, New York, 2007.
[2] G. Moody, PhysioNet: research resource for complex physiologic signals, Jpn. J. Electrocardiology 29 (2009) 1–3. ISSN: 0285-1660.
[3] E.A. Ashley, J. Niebauer, Cardiology explained, 2004.
[4] U.F. Chan, W.W. Chan, S.H. Pun, M.I. Vai, P.U. Mak, Flexible implementation of front-end bioelectric signal amplifier using fpaa for telemedicine system, in: Annual International Conference of the IEEE Engineering in Medicine and Biology—Proceedings, 2007, pp. 3721–3724.
[5] Y. Özbay, G. Tezel, A new method for classification of ECG arrhythmias using neural network with adaptive activation function, Digit. Signal Process. 20 (2010) 1040–1049.
[6] A. Pal, A.K. Gautam, Y.N. Singh, Evaluation of bioelectric signals for human recognition, Procedia Comput. Sci. 48 (2015) 746–752.
[7] J.G. Webster, Medical Instrumentation, Application and Design, fourth ed., Houghton Mifflin Company, Boston, 1978.
[8] S. Kara, Sensing of ECG signals and Imaging at the computer in real time (Ph.D. thesis), Erciyes University, 1991.
[9] C. Marek Malik, Guidelines heart rate variability standards of measurement, physiological interpretation, and clinical use, Eur. Heart J. Electrophysiol. (1996) 354–381.
[10] Y. Isler, M. Kuntalp, Combining classical HRV indices with wavelet entropy measures improves to performance in diagnosing congestive heart failure, Comput. Biol. Med. 37 (2007) 1502–1510.
[11] M. Jessup, S. Brozena, Heart failure, N. Engl. J. Med. 348 (2003) 2007–2018.
[12] D. Steinberg, A.M. Gotto, Preventing coronary artery disease by lowering cholesterol levels: fifty years from bench to bedside, JAMA 282 (1999) 2043–2050.
[13] J. He, L.G. Ogden, L.A. Bazzano, S. Vupputuri, C. Loria, P.K. Whelton, Risk factors for congestive heart failure in US men and women, Arch. Intern. Med. 161 (2001) 996.
[14] S. Baldasseroni, C. Opasich, M. Gorini, D. Lucci, N. Marchionni, M. Marini, et al., Left bundle-branch block is associated with increased 1-year sudden and total mortality rate in 5517 outpatients with congestive heart failure: a report from the Italian network on congestive heart failure, Am. Heart J. 143 (2002) 398–405.
[15] B. Gumus, S. Yazgi, Yapay sinir agi kullanilarak elektrokardiyogram sinyallerinde otomatik kardiyak aritmi tespiti, Elektrik Elektronik ve Bilgisayar Mühendisligi 13. Ulusal Kongresi, 2009.
[16] X.J.X. Jiang, L.Z.L. Zhang, Q.Z.Q. Zhao, S. Albayrak, ECG arrhythmias recognition system based on independent component analysis feature extraction, TENCON 2006 - 2006 IEEE Region 10 Conference, 2006.
[17] T.S. Lugovaya, Biometric human identification based on electrocardiogram (Master thesis), Electrotechnical University "LETI", 2005.
[18] Z. Dokur, T. Ölmez, ECG beat classification by a novel hybrid neural network, Comput. Methods Programs Biomed. 66 (2001) 167–181.
[19] S.A. Israel, J.M. Irvine, A. Cheng, M.D. Wiederhold, B.K. Wiederhold, ECG to identify individuals, Pattern Recognit. 38 (2005) 133–142.
[20] M. Kyoso, A. Uchiyama, Development of an ECG identification system, in: Annual Reports of the Research Reactor Institute, Kyoto University, volume 4, 2001, pp. 3721–3723.
[21] N. A.P., L. T.S, Biometric human identification based on electrocardiogram, XII-th Russian Conference on

Mathematical Methods of Pattern Recognition, 2005, pp. 387–390.
[22] S.C. Fang, H.L. Chan, Human identification by quantifying similarity and dissimilarity in electrocardiogram phase space, Pattern Recognit. 42 (2009) 1824–1831.
[23] T. Shen, W. Tompkins, Y. Hu, One-lead ECG for identity verification, Proceedings of the Second Joint 24th Annual Conference and the Annual Fall Meeting of the Biomedical Engineering Society [Engineering in Medicine and Biology 1], 2002.
[24] L. Biel, O. Pettersson, L. Philipson, P. Wide, ECG analysis: a new approach in human identification, IEEE Trans. Instrum. Meas. 50 (2001) 808–812.
[25] W. Yi, K. Park, D. Jeong, Personal identification from ECG measured without body surface electrodes using probabilistic neural networks, World Congress on Medical Physics and Biomedical Engineering, 2003.
[26] S. Bursíková, Application of Hilbert-Huang transform to the data of blood glucose profile, in: Student's Conference STC, 2007.
[27] F. Duman, N. Ozdemir, E. Yildirim, Patient specific seizure prediction algorithm using Hilbert-Huang Transform, in: Proceedings of 2012 IEEE-EMBS International Conference on Biomedical and Health Informatics, IEEE, 2012, pp. 705–708.
[28] V. Michal, Hilbert-Huang Transform, its features and application to the audio signal, in: Student's Conference STC, 2007.
[29] Y. Hou, H. Tian, An automatic modulation recognition algorithm based on HHT and SVD, in: Proceedings - 2010 3rd International Congress on Image and Signal Processing, CISP 2010, volume 8, 2010, pp. 3577–3581.
[30] U. Maji, M. Mitra, S. Pal, Automatic detection of atrial fibrillation using empirical mode decomposition and statistical approach, Procedia Technol. 10 (2013) 45–52.
[31] G. Altan, A. Yayik, Y. Kutlu, S. Yildirim, E. Yildirim, Analyse of congestive heart failure using Hilbert-Huang transform, DEU J. Sci. Eng. 16 (2014) 94–103. ISSN: 1302-9304
[32] J.P. Saul, Y. Arai, R.D. Berger, L.S. Lilly, W.S. Colucci, R.J. Cohen, Assessment of autonomic regulation in chronic congestive heart failure by heart rate spectral analysis, Am. J. Cardiol. 61 (1988) 1292–1299.
[33] G. Casolo, E. Balli, T. Taddei, J. Amuhasi, C. Gori, Decreased spontaneous heart rate variability in congestive heart failure, Am. J. Cardiol. 64 (1989) 1162–1167.
[34] P.F. Binkley, E. Nunziata, G.J. Haas, S.D. Nelson, R.J. Cody, Parasympathetic withdrawal is an integral component of autonomic imbalance in congestive heart failure: demonstration in human subjects and verification in a paced canine model of ventricular failure, J. Am. Coll. Cardiol. 18 (1991) 464–472.
[35] M. Asyali, Discrimination power of long-term heart rate variability measures, in: Proceedings of the 25th Annual International Conference of the IEEE Engineering in Medicine and Biology Society (IEEE Cat. No.03CH37439), IEEE, 2003, pp. 200–203.
[36] L. Pecchia, P. Melillo, M. Sansone, M. Bracale, Discrimination power of short-term heart rate variability measures for CHF assessment, IEEE Trans. Inf. Technol. Biomed. 15 (2011) 40–46.
[37] M. Engin, Spectral and wavelet based assessment of congestive heart failure patients, Comput. Biol. Med. 37 (2007) 820–828.
[38] U. Orhan, Real-time CHF detection from ECG signals using a novel discretization method, Comput. Biol. Med. 43 (2013) 1556–1562.
[39] Y.M. Akay, M. Akay, W. Welkowitz, J.L. Semmlow, J.B. Kostis, Noninvasive acoustical detection of coronary artery disease: a comparative study of signal processing methods, IEEE Trans. Biomed. Eng. 40 (1993) 571–578.
[40] K. Polat, S. Günes, S. Tosun, Diagnosis of heart disease using artificial immune recognition system and fuzzy weighted pre-processing, Pattern Recognit. 39 (2006) 2186–2193.
[41] I. Guler, E.D. Übeyli, Automated diagnostic systems with diverse and composite features for Doppler ultrasound signals, IEEE Trans. Biomed. Eng. 53 (2006) 1934–1942.
[42] U.R. Acharya, S.V. Sree, M. Muthu Rama Krishnan, N. Krishnananda, S. Ranjan, P. Umesh, et al., Automated classification of patients with coronary artery disease using grayscale features from left ventricle echocardiographic images, Comput. Methods Programs Biomed. 112 (2013) 624–632.
[43] H.G. Lee, K.Y.N. Noh, K.H. Ryu, A data mining approach for coronary heart disease prediction using HRV features and carotid arterial wall thickness, 2008 International Conference on BioMedical Engineering and Informatics 1, 2008.
[44] H.C.W. Kim, S. Jin, Y. Park, A study on development of multi-parametric measure of heart rate variability diagnosing cardiovascular disease, IFMBE Proc. 14 (2007) 3480–3483.
[45] D. Giri, U. Rajendra Acharya, R.J. Martis, S. Vinitha Sree, T.C. Lim, T. Ahamed, et al., Automated diagnosis of coronary artery disease affected patients using LDA, PCA, ICA and discrete wavelet transform, Knowl. Based Syst. 37 (2013) 274–282.
[46] A.L. Goldberger, L.A. Amaral, L. Glass, J.M. Hausdorff, P.C. Ivanov, R.G. Mark, et al., PhysioBank, PhysioToolkit, and PhysioNet: components of a new research resource for complex physiologic signals, Circulation 101 (2000) E215–E220.
[47] F. Jager, A. Taddei, M. Emdin, G. Antolic, R. Dorn, G. Moody, et al., The long-term ST database: a research resource for algorithm development and physiologic studies of transient myocardial ischemia, Comput. Cardiol. 27 (2000) (Cat. 00CH37163).
[48] P. Augustyniak, R. Tadeusiewicz, The Bandwidth variability of a typical electrocardiogram, in: European Medical and Biological Engineering Conference EMBEC 99, 1999, pp. 0–1.
[49] N.E. Huang, Z. Shen, S.R. Long, M.C. Wu, H.H. Shih, Q. Zheng, et al., The empirical mode decomposition and the Hilbert spectrum for nonlinear and non-stationary time series analysis, Proc. R Soc A 452 (1998) doi:10.1098/rspa.1998.0193.
[50] Y. Deng, W. Wang, C. Qian, D. Dai, Boundary-processing-technique in EMD method and Hilbert transform, Chin. Phys Lett 46 (2001) 954.
[51] Z. Yushan, L. Jianwen, H. Yuxian, Dealing with the boundary problem in EMD method by using autoregressive model, Prog. Nat. Sci. 13 (2003) 1054–1059.
[52] J. Wang, Y. Peng, X. Peng, Similarity searching based boundary effect processing method for empirical mode decomposition, Electron. Lett. 43 (2007) 58–59.
[53] M. Johanson, The Hilbert transform (Ph.D. thesis), Växjo University, Sweden, 1999.
[54] Z. Wu, N.E. Huang, Ensemble empirical mode decomposition: a noise-assisted data analysis method, Adv. Adapt. Data Anal. 1 (2009) 1–41.
[55] R.O. Duda, P.E. Hart, D.G. Stork, Pattern classification, 2000.
[56] D.E. Rumelhart, G.E. Hinton, R.J. Williams, Learning internal representations by error propagation, in: Parallel Distributed Processing: Explorations in the Microstructure of Cognition, volume 1, 1986, pp. 318–362.
[57] T.-T. Wong, Performance evaluation of classification algorithms by k-fold and leave-one-out cross validation, Pattern Recognit. 48 (2015) 2839–2846.
[58] W.J. Remme, Overview of the relationship between ischemia and congestive heart failure, Clin. Cardiol. 23 (2000) IV–4.